$B \to \pi l \nu$ Form Factors Calculated on the Light-Front

Chi-Yee Cheung,[a] **Chien-Wen Hwang,**[a,b] and **Wei-Min Zhang** [a]

[a]*Institute of Physics, Academia Sinica, Taipei 11529, Taiwan*

[b]*Department of Physics, National Taiwan University, Taipei 10764, Taiwan*

Abstract

A consistent treatment of $B \to \pi l \nu$ decay is given on the light-front. The B to π transition form factors are calculated in the entire physical range of momentum transfer for the first time. The valence-quark contribution is obtained using relativistic light-front wave functions. Higher quark-antiquark Fock-state of the B-meson bound state is represented effectively by the $|B^* \pi\rangle$ configuration, and its effect is calculated in the chiral perturbation theory. Wave function renormalization is taken into account consistently. The $|B^* \pi\rangle$ contribution dominates near the zero-recoil point ($q^2 \simeq 25$ GeV^2), and decreases rapidly as the recoil momentum increases. We find that the calculated form factor $f_+(q^2)$ follows approximately a dipole q^2-dependence in the entire range of momentum transfer.

PACS numbers: 13.20, 14.40.J

I. INTRODUCTION

The study of exclusive semileptonic decays of heavy mesons has attracted much interest in recent years. Semileptonic decays of heavy mesons to heavy mesons, such as $B \to D(D^*)l\nu$, provide an ideal testing ground for heavy-quark symmetry and heavy-quark effective theory. By comparison, weak decays of heavy mesons to light mesons are much more complicated theoretically, since in general there exists no symmetry principle for guidance. Nevertheless, it is essential to understand the reaction mechanisms of these decay modes, because they are the main sources of information on the CKM mixing matrix elements between heavy and light quarks. In particular, the study of the $B \to \pi l\nu$ decay is important for the determination of matrix element V_{ub} whose value is only poorly known [1].

Recently, the $B \to \pi l\nu$ decay has been investigated by many groups [2–17] using various different approaches, such as quark models, QCD sum rules, heavy-quark symmetry, perturbative QCD, and so on. In most studies, transition form factors are calculated only at one kinematic point, $q^2 = (P_B - P_\pi)^2 = 0$, so that extra assumptions are needed to extrapolate the form factors to cover the entire range of momentum transfer. In [13–16] chiral perturbation is employed, so that the results are valid for soft pion emission only. In [17] perturbative QCD is applied, in conjunction with hadronic wave functions obtained from QCD sum rule, to calculate the decay amplitudes; therefore the result is valid only when the final pion is energetic.

In this study, we first calculate the $B \to \pi l\nu$ decay form factors using relativistic light-front hadronic wave functions [Fig. (1a)]. The parameters in these wave functions are determined from other informations, and Melosh transformation is used to construct meson states of definite spins. Although light-front wave functions and quark model in the infinite momentum frame have been used in the past to study $B \to \pi l\nu$ decay and other heavy-light transitions [2,4,18], the decay form factors were only calculated for $q^2 = 0$. In this work, we directly evaluate for the first time the form factors in the entire kinematic region, so that additional extrapolation assumptions are no longer required. Secondly, we note that the $B \to \pi$ transition involves time-like momentum transfers. That means $q^+ \geq 0$ in the light-front coordinate, so that one must also consider the effects of the so-called nondiagonal light-front diagrams (or Z-graphs) [18–21], as depicted in Fig. (1b). These contributions are generated by the quark-antiquark ($q\bar{q}$) excitation or higher Fock-states in the hadronic

bound states. We shall effectively represent the $q\bar{q}$- configuration of the B-meson by the mesonic $|B^*\pi\rangle$ state, giving rise to the B^*-pole contribution shown in Fig. (1c). It was first noted by Isgur and Wise [22] that the B^*-pole effect is important in the zero-recoil region. Previous investigations either simply added this effect to the valence-quark contribution [22,23], or totally ignored it. In our more unified approach, the B^*-pole contribution arises from the $|B^*\pi\rangle$-component of the B-meson bound state. The mixing of different Fock-state configurations naturally requires a consistent wave function renormalization which has not been mentioned in all the previous works.

This paper is organised as follows. In Section II, the basic theoretical formalism is given. In Section III, numerical results are present and discussed, and finally a summary is given in Section IV.

II. GENERAL FORMALISM

The weak current that is responsible for b-quark decay is given by

$$J^\mu = \bar{q}\gamma^\mu(1 - \gamma_5)b, \tag{2.1}$$

where q stands for a light quark. For $B \to \pi l \nu$, only the vector current contributes, and our main task is to evaluate the hadronic matrix element, $M^\mu_{B\pi} = \langle\pi(P_\pi)|J^\mu|B(P_B)\rangle$, which can be parametrized as

$$
\begin{aligned}
M^\mu_{B\pi} &= \langle\pi(P_\pi)|J^\mu|B(P_B)\rangle \\
&= f_+(q^2)(P_B + P_\pi)^\mu + f_-(q^2)(P_B - P_\pi)^\mu.
\end{aligned} \tag{2.2}
$$

In the previous calculations of hadronic matrix elements in the infinite momentum frame or with light-front wave functions, one usually set $q^+ = P_B^+ - P_\pi^+ = 0$. This leads to $q^2 = -q_\perp^2$, implying a space-like momentum transfer. However, momentum transfers in real decay processes are always time-like. Hence matrix elements calculated with $q^+ = 0$ is relevant only at the maximum-recoil point with $q^2 = 0$, and one needs an extrapolation ansatz to extend the result to other physical momentum transfers. A direct calculation of the form factors for the whole momentum transfer range has not been performed. In this work, we work in a frame where the "$\perp$"- components of $\vec{P}_B$ and $\vec{P}_\pi$ vanish, so that $q^2 = q^+q^- \geq 0$, and we can evaluate the form factors in the entire physical range of momentum transfer. As

mentioned earlier, in a frame with $q^+ > 0$, there are two distinct contributions to the matrix element. Apart from the usual valence contribution [Fig. (1a)] which is calculated with relativistic light-front wave functions, one must also include the nondiagonal light-front diagram as depicted in Fig. (1b). Here, such non-valence effects are taken into account effectively by the B^*-pole contribution shown in Fig. (1c). Simple perturbation theory in the light-front approach gives [25]

$$|B(P_B)\rangle = \sqrt{Z_2}\left\{|B_0(P_B)\rangle + \int [d^3k][d^3q]\frac{\langle B^*(q)\pi(k)|H_I|B_0(P_B)\rangle}{P_B^- - q^- - k^-}|B^*(q)\pi(k)\rangle\right\}, \quad (2.3)$$

where $|B_0\rangle$ represents the valence configuration described by a light-front bound-state wave function, while $|B^* \pi\rangle$ is the most important higher-Fock-state configuration, as will be explained later; H_I is the interaction Hamiltonian for the $BB^*\pi$-vertex obtainable from chiral perturbation theory [13,14,24],

$$[d^3k] \equiv \frac{dk^+ d^2k_\perp}{2(2\pi)^3 k^+},$$
$$\langle P'|P\rangle = 2(2\pi)^3 P^+\delta(P'^+ - P^+)\delta^2(P'_\perp - P_\perp), \quad (2.4)$$

and $\sqrt{Z_2}$ is the wave function renormalization constant. All particles in Eq. (2.3) are on the mass-shells so that $P_B^- = \frac{P_{B\perp}^2 + M_B^2}{P_B^+}$, $q^- = \frac{q_\perp^2 + M_{B^*}^2}{q^+}$, and $k^- = \frac{k_\perp^2 + m_\pi^2}{k^+}$.

From Eqs. (2.2) and (2.3), we have formally

$$M_{B\pi}^\mu = \sqrt{Z_2}\left\{\left(f_+^v(q^2) + f_+^{B^*}(q^2)\right)(P_B + P_\pi)^\mu + \left(f_-^v(q^2) + f_-^{B^*}(q^2)\right)(P_B - P_\pi)^\mu\right\}, \quad (2.5)$$

where f_+^v, f_-^v represent the valence-configuration contributions, and $f_+^{B^*}, f_-^{B^*}$ the B^*-pole contributions. The resultant $B \to \pi l\nu$ decay form factors are therefore given by

$$f_+(q^2) = \sqrt{Z_2}\left[f_+^v(q^2) + f_+^{B^*}(q^2)\right],$$
$$f_-(q^2) = \sqrt{Z_2}\left[f_-^v(q^2) + f_-^{B^*}(q^2)\right]. \quad (2.6)$$

Most of the previous investigations only calculated $f_\pm^v$ at $q^2 = 0$, some also included the contribution of $f_\pm^{B^*}$, but none has taken into account the effect of $\sqrt{Z_2}$.

In the following, we shall first calculate the valence contribution using light-front bound state wave functions. Subsequently, the B^*-pole contribution, as well as the effect of wave function renormalization, will be discussed in more details.

A. Valence Configuration Contribution

A meson bound state consisting of a quark q_1 and an anti-quark $\bar{q}_2$ with total momentum P and spin S can be written as

$$|M(P, S, S_z)\rangle = \int \{d^3p_1\}\{d^3p_2\} \, 2(2\pi)^3\delta^3(\tilde{P} - \tilde{p}_1 - \tilde{p}_2)$$
$$\times \sum_{\lambda_1,\lambda_2} \Psi^{SS_z}(\tilde{p}_1, \tilde{p}_2, \lambda_1, \lambda_2) \, |q_1(p_1, \lambda_1)\bar{q}_2(p_2, \lambda_2)\rangle, \quad (2.7)$$

where p_1 and p_2 are the on-mass-shell light-front momenta,

$$\tilde{p} = (p^+, p_\perp), \quad p_\perp = (p^1, p^2), \quad p^- = \frac{m^2 + p_\perp^2}{p^+}, \quad (2.8)$$

and

$$\{d^3p\} \equiv \frac{dp^+ d^2p_\perp}{2(2\pi)^3}$$
$$|q(p_1, \lambda_1)\bar{q}(p_2, \lambda_2)\rangle = b^\dagger_{\lambda_1}(p_1)d^\dagger_{\lambda_2}(p_2)|0\rangle, \quad (2.9)$$
$$\{b_{\lambda'}(p'), b^\dagger_\lambda(p)\} = \{d_{\lambda'}(p'), d^\dagger_\lambda(p)\} = 2(2\pi)^3 \, \delta^3(\tilde{p}' - \tilde{p}) \, \delta_{\lambda'\lambda}.$$

In terms of the light-front relative momentum variables $(x, k_\perp)$ defined by

$$p_1^+ = x_1 P^+, \quad p_2^+ = x_2 P^+, \quad x_1 + x_2 = 1,$$
$$p_{1\perp} = x_1 P_\perp + k_\perp, \quad p_{2\perp} = x_2 P_\perp - k_\perp, \quad (2.10)$$

the momentum-space wave-function Ψ^{SS_z} can be expressed as

$$\Psi^{SS_z}(\tilde{p}_1, \tilde{p}_2, \lambda_1, \lambda_2) = R^{SS_z}_{\lambda_1\lambda_2}(x, k_\perp) \, \phi(x, k_\perp), \quad (2.11)$$

where $\phi(x, k_\perp)$ describes the momentum distribution of the constituents in the bound state, and $R^{SS_z}_{\lambda_1\lambda_2}$ constructs a state of definite spin (S, S_z) out of light-front helicity (λ_1, λ_2) eigenstates. Explicitly,

$$R^{SS_z}_{\lambda_1\lambda_2}(x, k_\perp) = \sum_{s_1,s_2}\langle\lambda_1|\mathcal{R}^\dagger_M(1 - x, k_\perp, m_1)|s_1\rangle\langle\lambda_2|\mathcal{R}^\dagger_M(x, -k_\perp, m_2)|s_2\rangle\langle\frac{1}{2}s_1\frac{1}{2}s_2|SS_z\rangle, \quad (2.12)$$

where $|s_i\rangle$ are the usual Pauli spinor, and $\mathcal{R}_M$ is the Melosh transformation operator:

$$\mathcal{R}_M(x, k_\perp, m_i) = \frac{m_i + x_i M_0 + i\vec{\sigma} \cdot \vec{k}_\perp \times \vec{n}}{\sqrt{(m_i + x_i M_0)^2 + k_\perp^2}}, \quad (2.13)$$

5

with $\vec{n} = (0, 0, 1)$, a unit vector in the z-direction, and

$$M_0^2 = \frac{m_1^2 + k_\perp^2}{x_1} + \frac{m_2^2 + k_\perp^2}{x_2}. \tag{2.14}$$

It is possible to rewrite the transformation matrix $R_{\lambda_1 \lambda_2}^{SS_z}$ in a covariant form [18], which is useful in practical calculations:

$$R_{\lambda_1 \lambda_2}^{SS_z}(x, k_\perp) = \frac{\sqrt{p_1^+ p_2^+}}{\sqrt{2} \, \tilde{M}_0} \, \bar{u}(p_1, s_1) \Gamma v(p_2, s_2), \tag{2.15}$$

where

$$
\begin{aligned}
&\tilde{M}_0 \equiv \sqrt{M_0^2 - (m_1 - m_2)^2}, \\
&\bar{u}(p, s) u(p, s') = \frac{2m}{p^+} \delta_{s,s'}, \quad \sum_s u(p, s) \bar{u}(p, s) = \frac{\slashed{p} + m}{p^+}, \\
&\bar{v}(p, s) v(p, s') = -\frac{2m}{p^+} \delta_{s,s'}, \quad \sum_s v(p, s) \bar{v}(p, s) = \frac{\slashed{p} - m}{p^+}, \\
&\Gamma = \gamma_5 \qquad \text{(pseudoscalar, } S = 0), \\
&\Gamma = -\slashed{\varepsilon}(S_z) + \frac{\varepsilon \cdot (p_1 - p_2)}{M_0 + m_1 + m_2} \qquad \text{(vector, } S = 1),
\end{aligned} \tag{2.16}
$$

with

$$
\begin{aligned}
&\varepsilon^\mu(\pm 1) = \left[\frac{2}{P^+} \vec{\varepsilon}_\perp(\pm 1) \cdot \vec{P}_\perp, 0, \vec{\varepsilon}_\perp(\pm 1) \right], \quad \vec{\varepsilon}_\perp(\pm 1) = \mp (1, \pm i)/\sqrt{2}, \\
&\varepsilon^\mu(0) = \frac{1}{M_0} \left(\frac{-M_0^2 + P_\perp^2}{P^+}, P^+, P_\perp \right),
\end{aligned} \tag{2.17}
$$

We normalize the meson state as

$$\langle M(P', S', S_z') | M(P, S, S_z) \rangle = 2(2\pi)^3 P^+ \delta^3(\tilde{P}' - \tilde{P}) \delta_{S'S} \delta_{S_z' S_z}, \tag{2.18}$$

so that

$$\int \frac{dx \, d^2 k_\perp}{2(2\pi)^3} \, |\phi(x, k_\perp)|^2 = 1. \tag{2.19}$$

In principle, the momentum distribution amplitude $\phi(x, k_\perp)$ can be obtained by solving the light-front QCD bound state equation [25,26]. However, before such first-principle solutions are available, we would have to be contented with phenomenological amplitudes. One example that has been often used in the literature for heavy mesons is the so-called BSW amplitude [2], which for a $B(b\bar{q})$-meson is given by

$$\phi_B(x, k_\perp) = \mathcal{N}_B \sqrt{x(1-x)} \, \exp\left(\frac{-k_\perp^2}{2\omega_B^2}\right) \, \exp\left[-\frac{M_B^2}{2\omega_B^2}(x-x_0)^2\right], \tag{2.20}$$

where $\mathcal{N}_B$ is the renormalization constant, x is the longitudinal momentum fraction carried by the light anti-quark, $x_0 = (\frac{1}{2} - \frac{m_b^2 - m_q^2}{2M_B^2})$, m_b=b-quark mass, m_q= light-quark mass, and ω_B is a parameter of order Λ_{QCD}.

For the pion, we shall adopt the Gaussian type wave function,

$$\phi_\pi(x, k_\perp) = \mathcal{N}_\pi \sqrt{\frac{dk_z}{dx}} \, \exp\left(-\frac{\vec{k}^2}{2\omega_\pi^2}\right), \tag{2.21}$$

where $\vec{k} = (k_\perp, k_z)$,

$$x = \frac{E_1 + k_z}{E_1 + E_2}, \qquad 1 - x = \frac{E_2 - k_z}{E_1 + E_2}, \tag{2.22}$$

with $E_i = \sqrt{m_i^2 + \vec{k}^2}$. We then have

$$M_0 = E_1 + E_2, \tag{2.23}$$

$$k_z = \left(x - \frac{1}{2}\right) M_0 - \frac{m_1^2 - m_2^2}{2M_0} \tag{2.24}$$

and

$$\frac{dk_z}{dx} = \frac{E_1 E_2}{x(1-x)M_0} \tag{2.25}$$

is the Jacobian of transformation from $(x, k_\perp)$ to $\vec{k}$. This wave function has been also used in many other studies of hadronic transitions. In particular, with appropriate parameters, it describes satisfactorily the pion elastic form factor up to $Q^2 \sim 10 \text{ GeV}^2$ [27].

With the light-front wave functions given above, and taking a Lorentz frame where $P_{B\perp} = P_{\pi\perp} = 0$ (i.e., $q_\perp = 0$), we readily obtain (for $B^0 \to \pi^+ l^- \bar{\nu}$)

$$\langle \pi(P_\pi)|J^\mu|B_0(P_B)\rangle = \sum_{\lambda's} \int \{d^3 p_d\} \phi_\pi^*(x', k_\perp) \phi_B(x, k_\perp)$$
$$\times R_{\lambda_u \lambda_d}^{00\dagger}(x', k_\perp) \, \bar{u}(p_u, \lambda_u) \gamma^\mu u(p_b, \lambda_b) R_{\lambda_b \lambda_d}^{00}(x, k_\perp), \tag{2.26}$$

where $x(x')$ is the momentum fraction carried by the spectator anti-quark ($\bar{d}$) in the initial(final) state, such that

$$xP_B^+ = x'P_\pi^+; \tag{2.27}$$

the meaning of all the other variables should be self obvious. The valence-quark part of the reaction mechanism is depicted in Fig. (1a). Substituting the covariant form given in Eq. (2.15) into Eq. (2.26), we get

$$\langle \pi(P_\pi)|J^\mu|B_0(P_B)\rangle = \sqrt{\frac{P_B^+}{P_\pi^+}} \int \frac{dx d^2 k_\perp}{2(2\pi)^3} \phi_\pi^*(x', k_\perp) \phi_B(x, k_\perp) \frac{-1}{2\tilde{M}_{0\pi}\tilde{M}_{0B}\sqrt{(1-x')(1-x)}}$$
$$\times \text{Tr}\left[\gamma_5(\not{p}_u + m_u)\gamma^\mu(\not{p}_b + m_b)\gamma_5(\not{p}_d - m_d)\right]. \tag{2.28}$$

The trace in the above expression can be easily carried out. For the "good" component, $\mu = +$, we get

$$- \text{Tr}\left[\gamma_5(\not{p}_u + m_u)\gamma^+(\not{p}_b + m_b)\gamma_5(\not{p}_d - m_d)\right]$$
$$= 4\left[\frac{m_q^2 + k_\perp^2}{x} + m_q(m_b - m_q)\right] P_\pi^+, \tag{2.29}$$

where we have set $m_u = m_d = m_q$. From Eq. (2.27), x and x' are related by $x = R_\pm x'$, with

$$R_\pm \equiv \frac{P_\pi^+}{P_B^+} = \frac{1}{2M_B^2}\left[M_B^2 + M_\pi^2 - q^2 \pm \sqrt{(M_B^2 + M_\pi^2 - q^2)^2 - 4M_B^2 M_\pi^2}\right]. \tag{2.30}$$

$R_\pm$ correspond to the pion recoiling in the positive and negative z-direction respectively relative to the B meson. The physical kinematic range $q^2 : 0 \rightarrow (M_B - M_\pi)^2$ corresponds to

$$R_+: 1 \rightarrow M_\pi/M_B,$$
$$R_-: (M_\pi/M_B)^2 \rightarrow M_\pi/M_B. \tag{2.31}$$

As pointed out in Ref. [26], the choice of the positive z-axis is immaterial, and the matrix elements calculated in both reference frames (call them the "+" and "−" frame) should produce the same form factors $f_\pm(q^2)$ as defined in Eq. (2.2). In the "+" frame, we write

$$f_+^v(q^2)(P_B^+ + P_\pi^+) + f_-^v(q^2)(P_B^+ - P_\pi^+) = F(R_+)P_\pi^+, \tag{2.32}$$

or equivalently,

$$f_+^v(q^2)(1 + R_+) + f_-^v(q^2)(1 - R_+) = F(R_+)R_+; \tag{2.33}$$

similarly, in the "−" frame,

$$f_+^v(q^2)(1 + R_-) + f_-^v(q^2)(1 - R_-) = F(R_-)R_-, \tag{2.34}$$

8

where

$$F(R_\pm) = \frac{\sqrt{R_\pm}}{(2\pi)^3} \int_0^1 dx' \int d^2k_\perp \phi_\pi^*(x', k_\perp) \phi_B(R_\pm x', k_\perp)$$

$$\times \frac{1}{\tilde{M}_{0\pi} \tilde{M}_{0B} \sqrt{(1-x')(1-R_\pm x')}} \left[\frac{m_q^2 + k_\perp^2}{R_\pm x'} + m_q(m_b - m_q) \right]. \tag{2.35}$$

Solving for $f_\pm^v(q^2)$ from Eqs. (2.33, 2.34), we finally arrive at

$$f_+^v(q^2) = \frac{F(R_+)R_+(1-R_-) - F(R_-)R_-(1-R_+)}{2(R_+ - R_-)} \tag{2.36}$$

and

$$f_-^v(q^2) = \frac{-F(R_+)R_+(1+R_-) + F(R_-)R_-(1+R_+)}{2(R_+ - R_-)}. \tag{2.37}$$

These are the valence-configuration contributions to the $B \to \pi l \nu$ decay form factors, valid in the entire range of momentum transfer $q^2 = [0, (M_B - M_\pi)^2]$.

B. Higher-Fock-State Contribution

It is often not adequate to describe the internal structure of a hadron solely by its valence configuration. As we have discussed, for time-like momentum transfers, one must also consider the effects of higher Fock-states corresponding to configurations containing quark-antiquark pairs in addition to the valence particles. Such contributions are shown in Fig. (1b). Unfortunately these higher-Fork-state wave functions are not available, and we shall estimate their contributions in an effective mesonic picture. In the case of the B-meson, it is expected that the effective higher-Fock-state configuration $|B^*\pi\rangle$ is the most important if the relative momentum is small. The reason is as follows. The B and B^* masses are almost degenerate due to heavy-quark symmetry, and also the pion mass is small. Consequently, when the relative momentum is small, the $|B^*\pi\rangle$ configuration is close to the energy shell (i.e., the energy denominator is small), and is thus enhanced. This can be readily seen in Eq.(2.3), where the interaction Hamiltonian H_I describing the $BB^*\pi$ coupling is given in chiral perturbative theory by [24]

$$H_I = -\frac{g}{f_\pi} \sqrt{M_B M_{B^*}} \int dx^- d^2x_\perp B_\mu^{*\dagger} (i\partial^\mu \pi^a) \tau^a B, \tag{2.38}$$

with $f_\pi = 93$ MeV being the pion decay constant.

9

The contribution to the decay matrix element from the $|B^*\pi\rangle$ configuration [see Fig. (1c)] is given by

$$\langle\pi(P_\pi)|J^\mu|B(P_B)\rangle_{B^*} = \int [d^3q]\langle 0|J^\mu|B^*(q)\rangle\frac{\langle B^*(q)\pi(P_\pi)|H_I|B_0(P_B)\rangle}{P_B^- - q^- - P_\pi^-}. \tag{2.39}$$

From

$$\langle 0|J^\mu|B^*(q)\rangle = M_{B^*}f_{B^*}\varepsilon^\mu, \tag{2.40}$$

$$\langle B^*(q)\pi^-(P_\pi)|H_I|B_0(P_B)\rangle = 2(2\pi)^3\delta^3(\tilde{P}_B - \tilde{q} - \tilde{P}_\pi)\frac{\sqrt{2}g}{f_\pi}\sqrt{M_B M_{B^*}}\;\varepsilon^*\cdot P_\pi, \tag{2.41}$$

and

$$\varepsilon^\mu\varepsilon^{*\nu} = -g^{\mu\nu} + \frac{P_{B^*}^\mu P_{B^*}^\nu}{M_{B^*}^2}, \tag{2.42}$$

we readily obtain

$$\langle\pi^-(P_\pi)|J^\mu|B(P_B)\rangle_{B^*} = \sqrt{2}g\frac{f_{B^*}}{f_\pi}\frac{P_{B^*}\cdot P_\pi P_B^\mu - (M_{B^*}^2 + P_{B^*}\cdot P_\pi)P_\pi^\mu}{P_{B^*}^+(P_B^- - P_{B^*}^- - P_\pi^-)}\sqrt{\frac{M_B}{M_{B^*}}}. \tag{2.43}$$

Therefore,

$$f_+^{B^*}(q^2) = g\frac{f_{B^*}}{\sqrt{2}f_\pi}\frac{-M_{B^*}^2}{P_{B^*}^+(P_B^- - P_{B^*}^- - P_\pi^-)}\sqrt{\frac{M_B}{M_{B^*}}} \tag{2.44}$$

$$f_-^{B^*}(q^2) = g\frac{f_{B^*}}{\sqrt{2}f_\pi}\frac{M_{B^*}^2 + 2P_{B^*}\cdot P_\pi}{P_{B^*}^+(P_B^- - P_{B^*}^- - P_\pi^-)}\sqrt{\frac{M_B}{M_{B^*}}} \tag{2.45}$$

where $P_{B^*}^+ = P_B^+ - P_\pi^+ > 0$ and $P_{B^*}^- = \frac{M_{B^*}^2 + (P_{B\perp} - P_{\pi\perp})^2}{P_B^+ - P_\pi^+}$. It is easy to see that $f_\pm^{B^*}$ are functions of q^2 because

$$\frac{1}{q^2 - M_{B^*}^2} = \frac{1}{P_{B^*}^+}\frac{1}{P_B^- - P_{B^*}^- - P_\pi^-} \qquad (q^+ = P_{B^*}^+). \tag{2.46}$$

However the above results are not quite complete, because chiral perturbation theory is a low-energy effective theory, such that the chiral $BB^*\pi$-vertex given in Eq. (2.38) is valid only for soft pions. A suppression factor is generally expected when the pion momentum increases. This can also be understood in the quark picture by the following reasoning. The higher Fock-state $|B^*\pi\rangle$ arises from quark-pair creation which is a predominently soft process. First of all, there is not much probability for producing hard $u\bar{u}$ pairs. Moreover, once produced, a hard u has little chance of forming a pion with a slow $\bar{u}$, likewise a hard $\bar{u}$ is not likely to form a B^*-meson with a slow b quark. Therefore configurations with a

high-momentum pion in $|B^*\pi\rangle$ is expected to be suppressed. This physical requirement can be implemented phenomenologically by introducing a damping form factor, $\mathcal{F}(q^2)$, to the chiral $BB^*\pi$-vertex, such that,

$$g \to g\mathcal{F}(q^2). \tag{2.47}$$

We shall take

$$\mathcal{F}(q^2) = \exp\left(-\frac{v_B \cdot (p_\pi - M_\pi)}{\Lambda}\right), \tag{2.48}$$

where $v_B = P_B/M_B$ is the 4-velocity of the B-meson, and Λ is the cutoff momentum which is expected to be of the order of the chiral symmetry breaking scale $\Lambda_\chi \simeq 1$ GeV. The form of the suppression factor is similar to that proposed by Wolfenstein [15] in the soft-pion region, and is normalized to unity at the zero-recoil point where $q^2 = (M_B - M_\pi)^2$. The substitution indicated in Eq. (2.47) is to be understood for all of the equations derived in this Subsection.

C. Wave Function Renormalization

Finally we calculate the wave function renormalization constant Z_2 which is required for consistency, as indicated in Eq. (2.3). The result is

$$Z_2^{-1} = 1 + \frac{1}{2(2\pi)^3 P_B^+} \int [d^3k][d^3q] \frac{|\langle B^*(q)\pi(k)|H_I|B_0(P_B)\rangle|^2}{(P_B^- - q^- - k^-)^2}$$
$$= 1 + \frac{3g^2}{f_\pi^2} \frac{M_B M_{B^*}}{P_B^+} \int [d^3q] \frac{1}{k^+} \frac{[\varepsilon \cdot k]^2}{[P_B^- - q^- - k^-]^2} \mathcal{F}^2[(P_B - k)^2], \tag{2.49}$$

where q and k are on the mass-shells, $k^+ = P_B^+ - q^+$, $k_\perp = -q_\perp$, and we have included the suppression form factor as given in Eqs. (2.47, 2.48).

Combining Eqs. (2.36), (2.37), (2.44), (2.45) and (2.49) together, we obtain a relatively more consistent treatment for $B \to \pi l\nu$ decay form factors in comparison to the previous studies.

III. NUMERICAL RESULTS

In this section, we present the numerical results for $B \to \pi l\nu$ decay form factors. We first present contributions from the valence-quark configuration. The parameters in the

light-front wave functions are fixed by fitting to other hadronic properties. For the pion wave function, the parameters ω_π and $m_q(= m_{u,d})$ are fitted to the pion decay constant f_π and also the pion elastic form factor for momentum transfer $Q^2 = 0 \sim 10$ GeV^2 [27]:

$$\omega_\pi = 0.29 \text{ GeV}, \quad m_q = 0.30 \text{ GeV}. \tag{3.1}$$

For the light-front B-meson wave function, we take

$$\omega_B = 0.57 \text{ GeV}, \quad m_b = 4.8 \text{ GeV}, \tag{3.2}$$

which were determined from the B decay constant $f_B = 0.187$ GeV, and other decay data [2,28]. With these parameters, the decay form factor f_+^v due to the valence configuration is presented in Fig. (2). At the maximum recoil point $(q^2 = 0)$,

$$f_+^v(0) = 0.24, \tag{3.3}$$

which is consistent with results from most other calculations [2–12,17]. A slightly different set of parameters for the pion wave function

$$\omega_\pi = 0.33 \text{ GeV}, \quad m_q = 0.25 \text{ GeV} \tag{3.4}$$

also fits the pion data quite well. The result is not qualitatively changed by using this set of numbers, as can be seen also in Fig. (2). The value of the form factor at $q^2 = 0$ is however increased by 20% to

$$f_+^v(0) = 0.29. \tag{3.5}$$

It is a common practice in the literature to extrapolate $f_+(q^2)$ away from the $q^2 = 0$ point by a monopole q^2-dependence, even though such a q^2-dependence is expected to be reasonable only near the zero-recoil point $[q^2 = (M_B - M_\pi)^2]$. Our result does not confirm such a q^2-dependence. Instead, as shown in Fig. (4), for a wide range of momentum transfer, $q^2 = 0 \sim 18$ GeV^2, the valence contribution agrees rather well with the following formula:

$$f_+^{pole}(q^2) = \frac{f_+(0)}{(1 - q^2/M_{pole}^2)^\alpha}, \tag{3.6}$$

with $\alpha = 1.6$ and $M_{pole} = 5.32$ GeV.

From Fig. (2), we see that, near the zero-recoil point, the valence-quark prediction decreases as q^2 increases, and no longer bears any resemblence to Eq. (3.6). The dipping of

the valence-quark contribution toward the zero-recoil point can be understood as follows. Recall that the decay amplitude involves an overlapping integral of the wave functions of the initial and final mesons. If both mesons were heavy, then it is obvious that, by heavy-quark symmetry, maximum overlapping must occur at the zero-recoil point. However, in the present situation, a heavy (B) and a light meson (π) are involved, and their internal momentum distributions peak at different values of x. Specifically, $\phi_B(x, k_\perp)$ has a narrow peak near $x = 0$, whereas $\phi_\pi(x, k_\perp)$ peaks with a much larger width at $x = 1/2$. Consequently maximum overlapping of the wave functions actually occurs somewhat away from the zero-recoil kinematics.

To test the sensitivity to the B-meson wave function used, we plot in Fig. (3) the valence contribution, using a Gaussian wave function of the same form as shown in Eq. (2.21), with $\omega_B = 0.73$ GeV. We find that the result is not changed significantly except in the zero-recoil region, $q^2 > 20$ GeV^2. As we shall see, in the zero-recoil region, the B^*-pole contribution dominates, and the valence contribution is relatively not important.

Next we consider the B^*-pole (or higher-Fock-state) contribution given by Eqs. (2.44, 2.45). We take

$$f_B = 0.187 \text{ GeV}, \quad f_{B^*}/f_B = 1.1, \quad g = 0.48, \quad \Lambda = 1.0 \text{ GeV}, \tag{3.7}$$

where the values taken for f_B and the ratio f_B/f_{B^*} are consistent with QCD sum rule and lattice QCD results [11,29,30]. However the magnitude of g is less certain; it is not directly measurable, since $B^* \to B\pi$ is kinematically forbidden. In the infinite-heavy-quark-mass limit, heavy-quark symmetry predicts that g is independent of heavy quark flavor, so that $BB^*\pi$ is equal to $DD^*\pi$ which is experimentally measurable. However,they have different $1/m_Q$ corrections. From the upper limit of the total width of $D^{*+}(< 131$ MeV) [31], we know that, g should be less than 0.7. From non-relativistic quark-model constrained by the axial coupling constant $g_A = 1.25$ of the nucleon, one gets [24,32] $g = 0.75$ in the symmetry limit, which some what overshoots the experimental upper limit. QCD-sum-rule calculations [33–35] usually obtain smaller values, namely, $g \simeq 0.2 \sim 0.4$. Results from various other approaches tend to fall between these two limits [28,36–39]. In Eq. (3.7), we have simply taken the average of the non-relativistic quark model prediction and the lowest of the QCD sum-rule results. The cutoff momentum Λ in Eq. (2.47) is also not well known, and we have assumed Λ to be equal to the chiral symmetry breaking scale $\Lambda_\chi \simeq 1$ GeV. Sensitivity of

13

the results to the values of g and Λ will be shown below.

Finally, we need to compute the renormalization constant Z_2 given by Eq. (2.49). The result is $\sqrt{Z_2} = 0.85, 0.93, 0.98$, for $g = 0.75, 0.48, 0.20$ respectively. Hence, depending on the coupling constant g, the effect of wave function renormalization can be quite significant (2-15%).

The B^*-pole contribution is plotted in Fig. (5a) with $\Lambda = 1.0$ GeV and three values of g as indicated. The combined valence and B^*-pole contribution is plotted in Fig. (5b). We see that the B^*-pole contribution dominates in the zero-recoil region, $q^2 \simeq 25$ GeV^2, and decreases rapidly as q^2 decreases. With the B^*-contribution included, we find $f_+(0) = 0.26, 0.28, 0.29$ for $g = 0.20, 0.48, 0.75$ respectively; therefore the effect of the B^* contribution at $q^2 = 0$ is within the theoretical error caused by the uncertainty in the pion wave function [see Eqs. (3.3, 3.5)]. For $g = 0.48$, the theoretical result can be approximately described by Eq. (3.6), with $\alpha = 2.0$ and $M_{pole} = 6.0$ GeV [see Fig. (6a)]. The $g = 0.2$ curve also shows approximately a dipole behavior ($\alpha = 2.0$), with a slightly different pole mass $M_{pole} = 5.8$ GeV [see Fig. (6b)]. Hence our results indicate that $f_+(q^2)$ does not follow a simple monopole q^2-dependence (i.e. $\alpha = 1.0$).

In order to study the sensitivity of our results to the cut-off parameter Λ, we have plotted in Fig. (7) the same curves as in Fig. (5b), but with Λ=1.5 GeV. From Eqs. (2.44,2.47,2.48), it is easily seen that the B^*-pole contribution $f_+^{B^*}$ increases with Λ; this effect is however counter balanced by a smaller Z_2. Since we have taken into account the effect of wave function renormalization, our results are relatively insensitive to the precise value of Λ used. It thus seems that a measurement of $f_+(q^2)$ near zero-recoil would give a rather good estimate of the $BB^*\pi$ coupling constant g, which is not obtainable from direct strong decays.

IV. SUMMARY

The exclusive $B \to \pi l \nu$ decay is studied in this paper. We have calculated two different contributions to the decay process: The valence-quark contribution is calculated using light-front wave functions for mesons, while the B^*-pole contribution is evaluated with the help of chiral perturbation theory. In contrast to previous works using relativistic wave functions, the decay form factors have been calculated directly in the entire range of mo-

mentum transfer, so that extrapolation from $q^2 = 0$ is no longer required. Furthermore, in a more unified approach, the B^*-pole contribution is calculated from the higher-Fock-state configuration $|B^*\pi\rangle$ of the B-meson wave function. The mixing of different configurations requires a consistent renormalization of the B-meson wave function, which is a 7% effect for g=0.48; 2% if g=0.2. We find that the form factor $f_+(q^2)$ does not follow a monopole q^2-dependence, as is customarily assumed in the literature. Instead, our result is closer to a dipole q^2-dependence. At the maximum recoil point, we find that $f_+(0) = 0.24 - 0.29$, which is consistent with most other calculations. Finally we observe that, since the B^*-pole contribution dominates in the zero-recoil region, a measurement of $f_+(q^2)$ near zero-recoil would be helpful in determining the value of the chiral $BB^*\pi$ coupling constant g.

REFERENCES

[1] Particle Data Group, Phys. Rev. D **50**, 1315 (1994).

[2] M. Wirbel, S. Stech, and M. Bauer, Z. Phys. C **29**, 637 (1985); M. Bauer and M. Wirbel, *ibid.* **42**, 671 (1989).

[3] N. Isgur, D. Scora, B. Grinstein, and M. Wise, Phys. Rev. D **39**, 799 (1989).

[4] P.J. O'Donnell, Q.P. Xu, and K.K. Tung, Preprint UTPT-95-2 (Univ. of Toronto).

[5] R.N. Faustov, V.O. Galkin, and a. Yu. Mishurov, Preprint (Russian Academy of Science).

[6] P. Ball, V.M. Braun, H.G. Dosch, Phys. Lett. B **273**, 316 (1991); Phys. Rev. D **44**, 3567 (1991); P. Ball, Phys. Rev. D **48**, 3190 (1993).

[7] V.L. Chernyak and I.R. Zhitnitsky, Nucl. Phys. B **345**, 137 (1990); A.A. Ovchinnikov, Sov. J. Nucl. Phys. **50**, 519 (1989); C.A. Dominguez and N. Paver, Z. Phys. C **41**, 217 (1988).

[8] V.M. Belyaev, A. Khodjamirian, and R. Rückl, Z. Phys. C **60**, 349 (1993).

[9] P. Colangelo and P. Santorelli, Phys. Lett. B **327**, 123 (1994).

[10] A. Ali, V. M. Braun, and H. G. Dosch, Z. Phys. C **63**, 437 (1994).

[11] H.Y. Cheng, Chin. J. Phys. **32**, 425 (1994).

[12] G. Burdman, Z. Ligeti, M. Neubert, and Y. Nir, Phys. Rev. D **49**, 2331 (1994).

[13] M.B. Wise, Phys. Rev. D **45**, 2188 (1992).

[14] G. Burdman and J.F. Donoghue, Phys. Lett. B **280**, 287 (1992).

[15] L. Wolfenstein, Phys. Lett. B **291**, 177 (1992).

[16] R. Casalbuoni, A. Deandrea, N. Di Bartolomeo, R. Gatto, F. Feruglio, and G. Nardulli, Phys. Lett. B **299**, 139 (1993).

[17] H.N. Li and H.L. Yu, Phys. Rev. Lett. **74**, 4388 (1995).

[18] W. Jaus, Phys. Rev. D **41**, 3394 (1990).

[19] S.J. Brodsky, Private communication.

[20] M. Sawicki, Phys. Rev. D **44**, 433 (1991).

[21] A. Dubin and A. Kaidalov, Yad. Fiz. **56**, 164 (1993), [Phys. At. Nucl. **56**, 237 (1993)].

[22] N. Isgur and M. B. Wise, Phys. Rev. D **41**, 151 (1990).

[23] G. Burdman and J. F. Donoghue, Phys. Rev. Lett. **68**, 2887 (1992).

[24] T.M. Yan, H.Y. Cheng, C.Y. Cheung, G.L. Lin, Y.C. Lin, and H.L. Yu, Phys. Rev. D **46**, 1148 (1992).

[25] W. M. Zhang, Chinese. J. Phys. **31**, 717 (1994); Preprint IP-ASTP-19-95 (hep-ph/9510428).

[26] C.Y. Cheung, W.M. Zhang, and G.L. Lin, Phys. Rev. D **52**, 2915 (1995).

[27] P.L. Chung, F. Coester, and W.N. Polyzou, Phys. Lett. B **205**, 545 (1988).

[28] P.J. O'Donnell and Q.P. Xu, Phys. Lett. B **336**, 113 (1994).

[29] M. Neubert, Phys. Rev. D **46**, 1076 (1992).

[30] A. Abada, et al., Nucl. Phys. B **376**, 172 (1992).

[31] S. Barlarg et al., Phys. Lett. B **278**, 480 (1992).

[32] H.Y. Cheng, C.Y. Cheung, G.L. Lin, Y.C. Lin, T.M. Yan, and H.L. Yu, Phys. Rev. D **49**, 5857 (1994).

[33] T.M. Aliev, D.A. Demir, E. Iltan, and N.K. Pak, Phys. Lett. B **351**, 339 (1995).

[34] P. Colangelo, G. Nardulli, A. Deandrea, N. di Bartolomeo, R.Gatto, and F. Fergulio, Phys. Lett. B **339**, 151 (1994).

[35] V.M. Belyaev, V.M. Braun, A. Khodjamirian, and R. Rückl, Preprint (MPI-PhT/94-62).

[36] P. Cho and H. Georgi, Phys. Lett. B **296**, 408 (1992).

[37] J.F. Amundson et al., Phys. Lett. B **296** 415 (1992).

[38] W.A. Bardeen and C.T. Hill, Phys. Rev. D **49**, 409 (1994).

[39] E. Eichten et al., Phys. Rev. D **21**, 203 (1988).

FIGURE CAPTIONS

Fig. (1a) $B \to \pi l \nu$: Valence-quark contribution.

Fig. (1b) $B \to \pi l \nu$: Non-valence contribution.

Fig. (1c) $B \to \pi l \nu$: B^*-pole contribution.

Fig. (2) Valence-quark contribution to $f_+(q^2)$. Solid line: $m_q = 0.30$ GeV, $\omega_\pi = 0.29$ GeV; dashed line: $m_q = 0.25$ GeV, $\omega_\pi = 0.33$ GeV.

Fig. (3) Solid line: Same as that in Fig. (2); dashed line: Gaussian wave function used for B, with $\omega_B = 0.73$ GeV.

Fig. (4) Solid line: Same as that in Fig. (2); dashed line: Eq. (3.6), with $\alpha = 1.6$ and $M_{pole} = 5.32$ GeV.

Fig. (5a) Solid lines: B^*-pole contribution with $\Lambda = 1$ GeV; dashed line: valence-quark contribution [same as solid line in Fig. (2)].

Fig. (5b) Combined valence-quark and B^*-pole contribution with $\Lambda = 1$ GeV.

Fig. (6a) Solid line: same as the $g = 0.48$ line in Fig. (5b); dashed line: Eq. (3.6) with $\alpha = 2.0$ and $M_{pole} = 6.0$ GeV; dash-dotted line: Eq. (3.6) with $\alpha = 1.0$ and $M_{pole} = 5.32$ GeV.

Fig. (6b) Solid line: $g = 0.20$ line from Fig. (5b); dashed line: Eq. (3.6) with $\alpha = 2.0$ and $M_{pole} = 5.8$ GeV; dash-dotted line: Eq. (3.6) with $\alpha = 1.0$ and $M_{pole} = 5.32$ GeV.

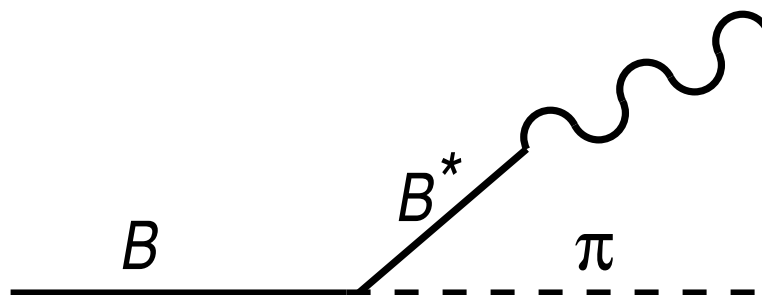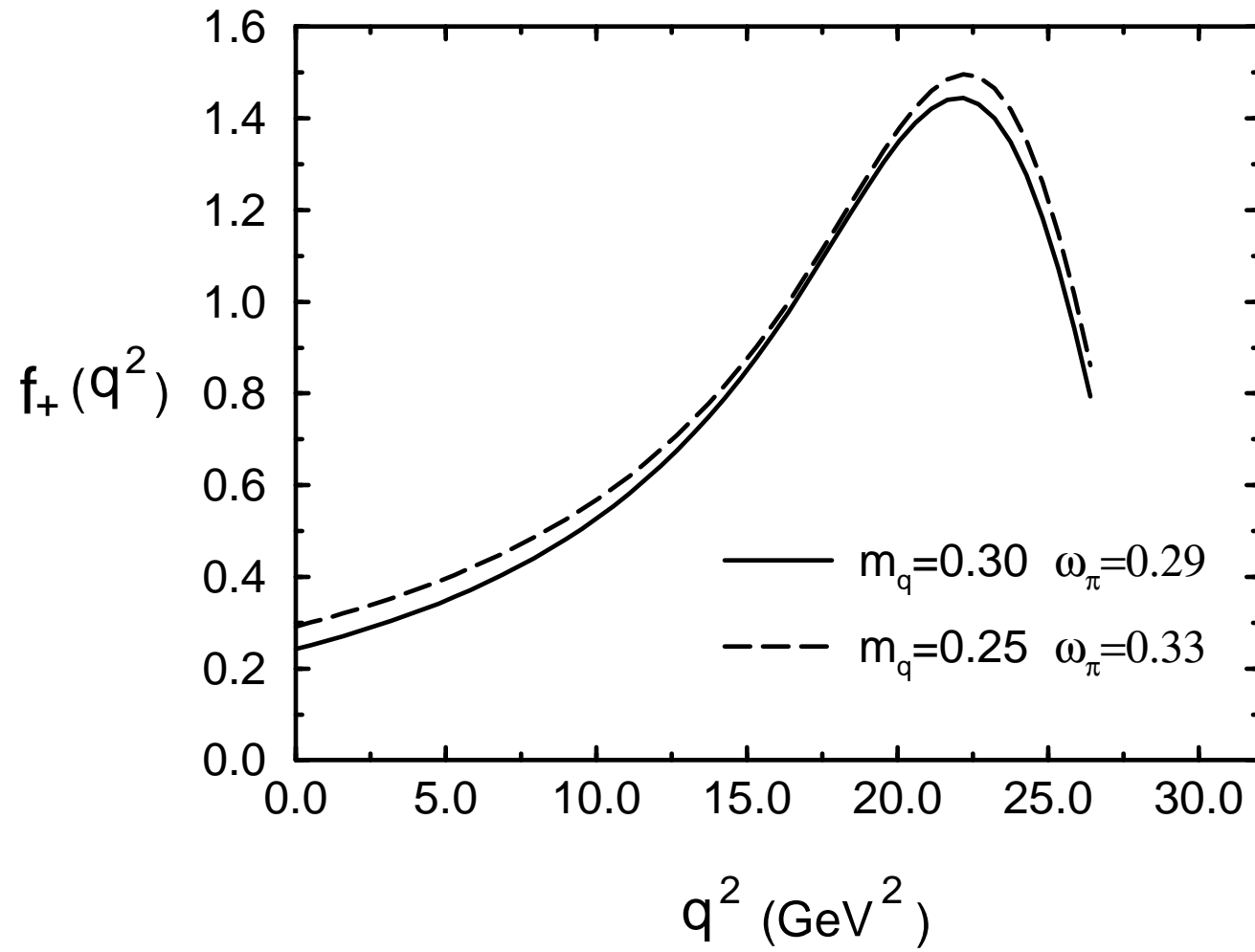**Fig. (7)** Same as Fig. (5b) except that $\Lambda = 1.50$ GeV

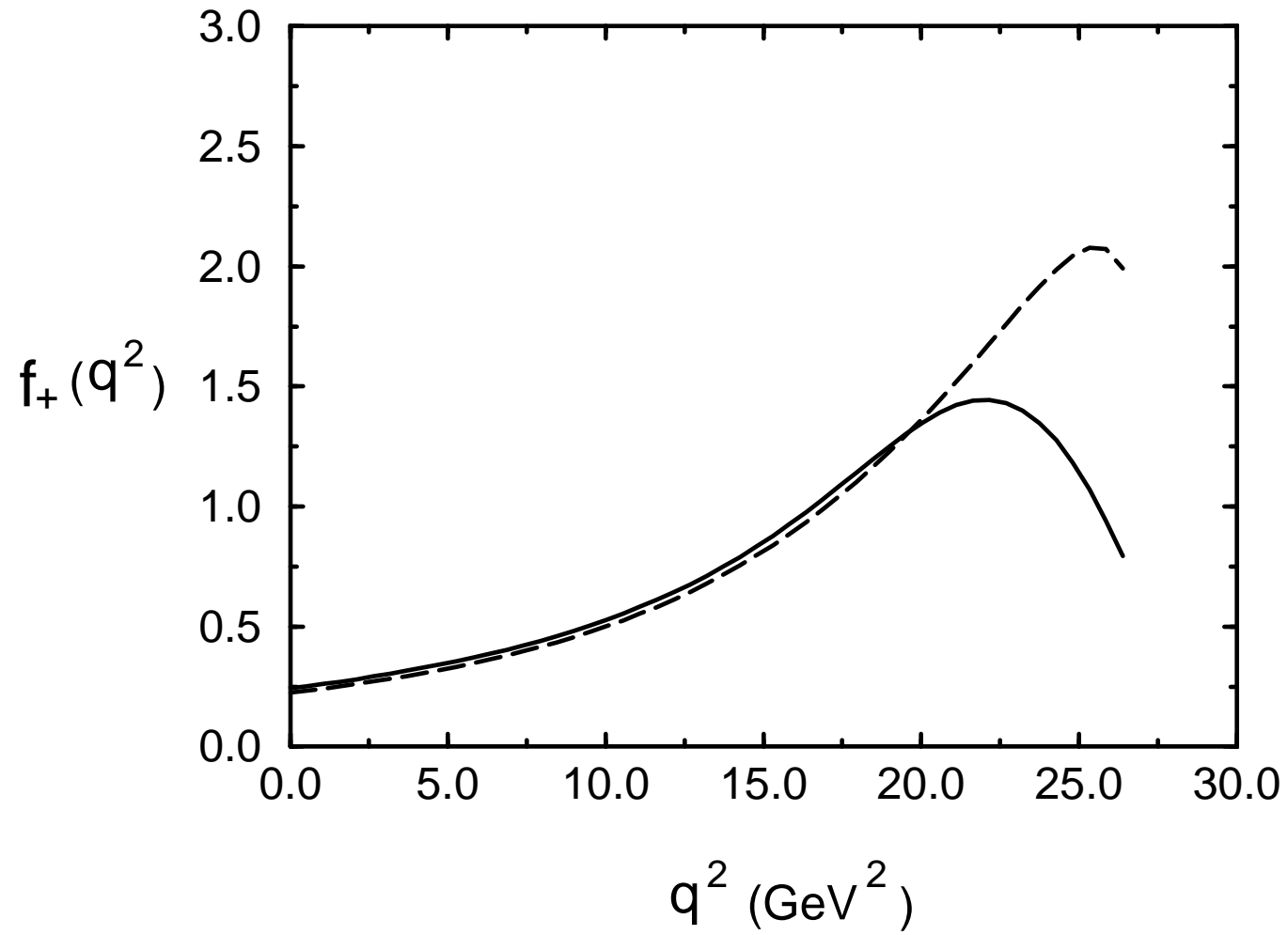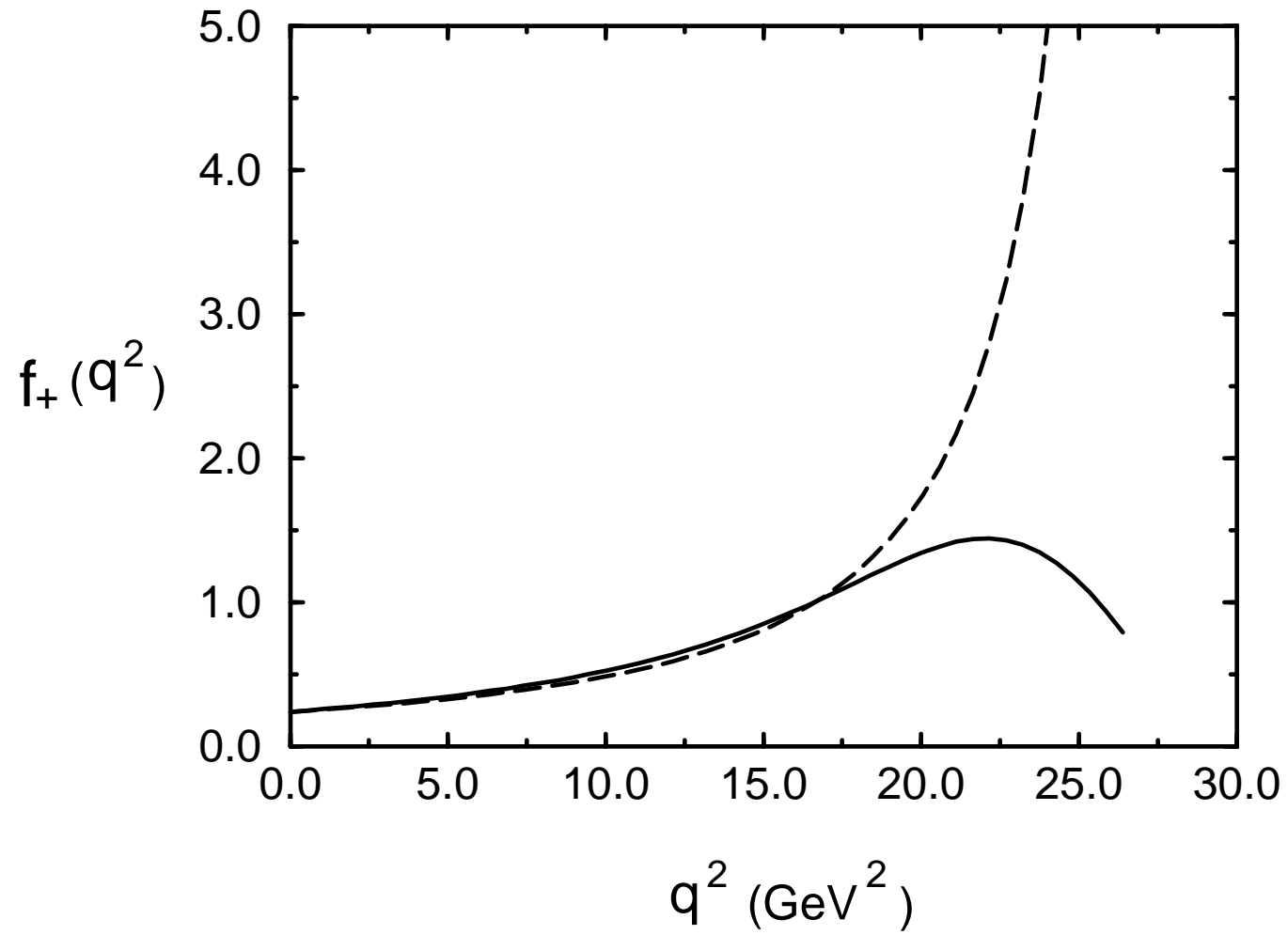# Fig.1
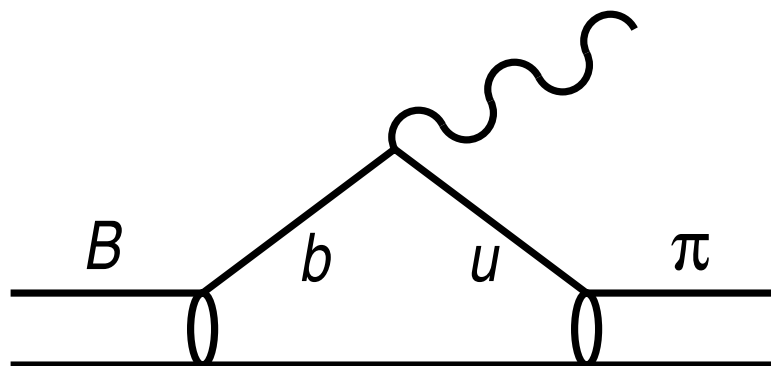
(a)
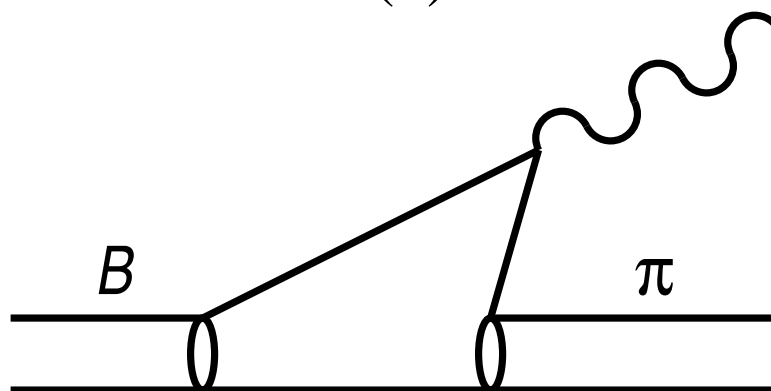
(b)

(c)

Fig. 2

Fig. 3

Fig. 4

Fig. 5(a)

Fig. 5(b)
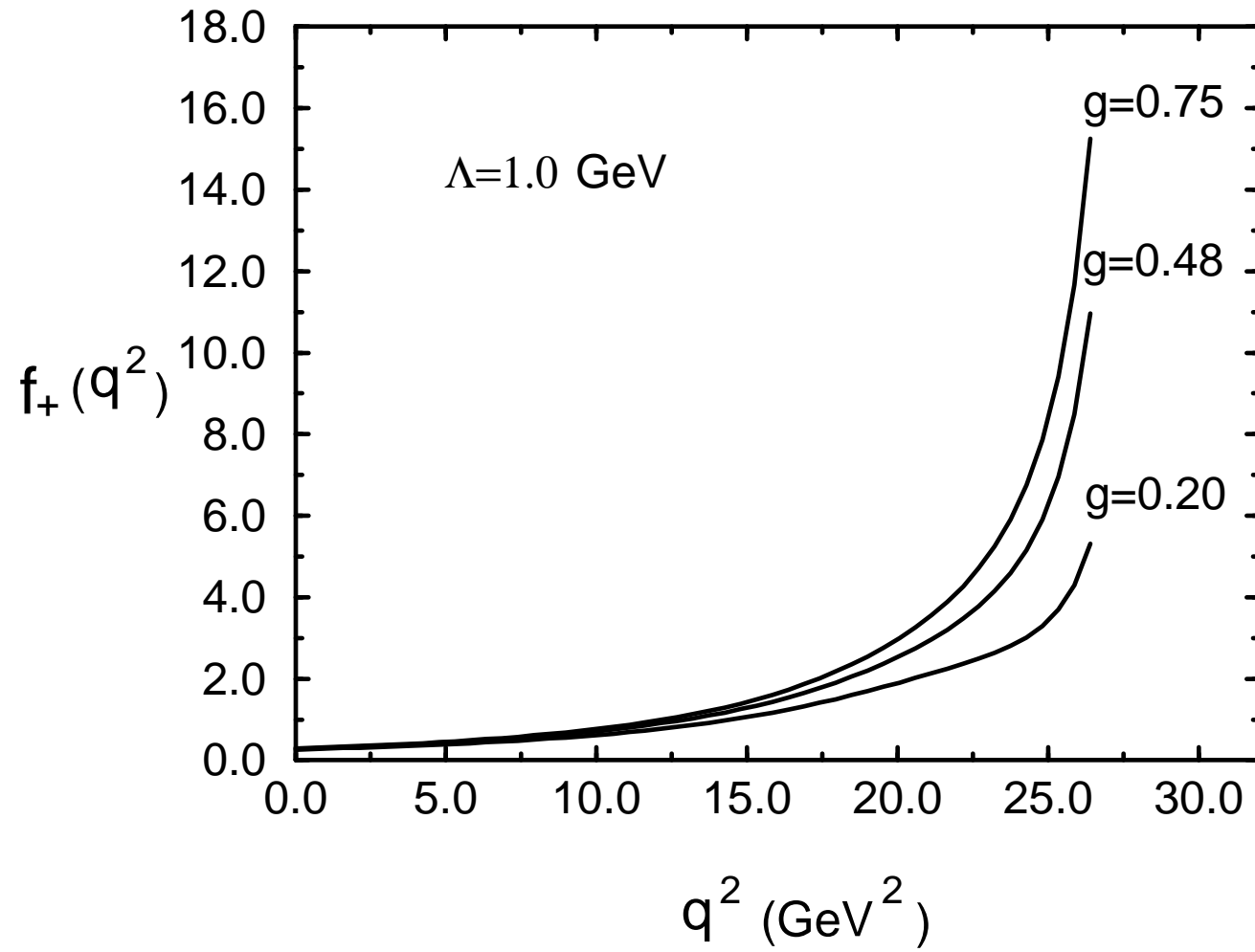
Λ=1.0 GeV

g=0.75

g=0.48

g=0.20

$f_+(q^2)$

q^2 (GeV^2)

Fig. 6(a)

Fig. 6(b)

g=0.20, Λ=1.0 GeV

$f_+(q^2)$

q^2 (GeV^2)

Fig. 7